JOURNAL OF MATERIALS SCIENCE 21 (1986) 3638–3642

Correlation of burst pressure of GRP cylinders with the stress wave factor

V. K. SRIVASTAVA
Department of Mechanical Engineering, Institute of Technology, Banaras Hindu University, Varanasi-221 005, India

Glass fibre-reinforced plastic (GRP) cylinders are increasingly used for highly stressed structural elements. The higher the demands on the materials, the higher are the fault detection requirements to be met by non-destructive materials testing methods. Acousto-ultrasonics is a valuable aid for the non-destructive evaluation of GRP composite materials, because it may be the answer to evaluating effects of subtle defects in composites. The aim of the research is to evaluate the burst pressure of GRP cylinders by acousto-ultrasonics techniques. The theoretical results have been found to be in good agreement with the experimental values. Hence the results strongly suggest that stress wave factor measurements can be exploited successfully to predict burst pressure of GRP cylinders.

Nomenclature

P	Internal pressure, kgf cm^{-2}
d	Internal diameter, cm
t	Thickness of cylinder, cm
$(N_x, N_\theta, N_{x\theta})$	Resultant forces, kgf
$(M_x, M_\theta, M_{x\theta})$	Moments, kg cm
$[A]$	Extensional stiffness matrix
$[B]$	Bending stretching coupling matrix
$[D]$	Flexural stiffness matrix
$(\varepsilon_x^0, \varepsilon_\theta^0, \varepsilon_{x\theta}^0)$	Midplane strains
$(k_x, k_\theta, k_{x\theta})$	Curvatures
n	Number of laminae
Z	Distance from midplane, cm
σ_u	Ultimate tensile strength of GRP composite, kg cm^{-2}
S_w	Stress wave factor
m	Material parameter
ϕ	Filament winding angle

1. Introduction

Glass fibre-reinforced plastic cylinders are increasingly used in industrial environments, where their strength, low weight and corrosion resistance make them competitive with other materials. However, for most load-bearing applications, the short-term properties cannot be used as a basis for design calculations without some knowledge of the critical limits for failure. Hence a suitable non-destructive evaluation (NDE) method could be developed to evaluate the internal features of the GRP composites and provide a measure which, in turn, may be related to the burst pressure of GRP cylinders. The composite laminate failure was affected by different factors such as constituent strength and moduli lamination orientations, flaw populations and distributions, applied and residual stresses, energy dissipation, dynamics and fracture propagation paths [1].

A new technique (acousto-ultrasonics) involving the use of an ultrasonic sensor to inject a stress pulse into the specimen, and a lower frequency acoustic emission sensor to receive the transformed wave form, has been found to characterize the energy dissipation dynamics. This technique has been found to assess the integrated effect of flaw population as well as the subtle effects. The stress wave factor is arbitrary and depends on factors such as probe pressure, coupling, signal gain, reset time, threshold voltage, repetition rate [2–4]. Schwalbe [5] has carried out a study of defects in GRP cylinders by acoustic emission technique. Several investigators have tried to develop relations to predict the behaviour of fibre-reinforced plastic composites by the stress wave factor [6–8].

The present paper describes the relationship between stress wave factor and burst pressure of GRP composite cylinders.

2. Theoretical work

A filament-wound cylinder consists of several layers of filament winding at $\pm\phi$. These layers interact and may not be symmetrical around the midplane. The integrated stress–strain and moment curvature relations for the filament-wound cylinder, which are also known as constitutive relations, are given as:

$$\begin{bmatrix} N_x \\ N_\theta \\ N_{x\theta} \\ M_x \\ M_\theta \\ M_{x\theta} \end{bmatrix} = \begin{bmatrix} A_{11} & A_{12} & A_{16} & B_{11} & B_{12} & B_{16} \\ A_{21} & A_{22} & A_{26} & B_{21} & B_{22} & B_{26} \\ A_{61} & A_{62} & A_{66} & B_{61} & B_{62} & B_{66} \\ B_{11} & B_{12} & B_{16} & D_{11} & D_{12} & D_{16} \\ B_{21} & B_{22} & B_{26} & D_{21} & D_{22} & D_{26} \\ B_{61} & B_{62} & B_{66} & D_{61} & D_{62} & D_{66} \end{bmatrix} \begin{bmatrix} \varepsilon_x^0 \\ \varepsilon_\theta^0 \\ \varepsilon_{x\theta}^0 \\ k_x \\ k_\theta \\ k_{x\theta} \end{bmatrix} \quad (1)$$

$$A_{ij} = \sum_{k=1}^{n} (\bar{Q}_{ij})_k (h_k - h_{k-1}) \quad (2)$$

0022–2461/86 $03.00 + .12

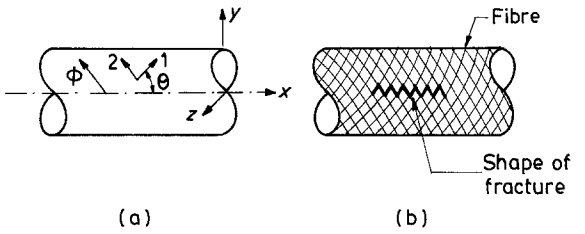

Figure 1 (a) Relationship between lamina principle axes (1, 2) and reference axes (x, y, z). (b) Fractured specimen of GRP cylinder.

$$B_{ij} = \frac{1}{2}\sum_{k=1}^{n}(\bar{Q}_{ij})_k(h_k^2 - h_{k-1}^2) \quad (3)$$

$$D_{ij} = \frac{1}{3}\sum_{k=1}^{n}(\bar{Q}_{ij})_k(h_k^3 - h_{k-1}^3) \quad (4)$$

The terms (N_x, N_θ, $N_{x\theta}$) are the resultant forces, (M_x, M_θ, $M_{x\theta}$) are the moments, [A] is the extensional stiffness matrix, [B] is the bending stretching coupling matrix, [D] is the flexural stiffness matrix, (ε_x^0, ε_θ^0, $\varepsilon_{x\theta}^0$) are the midplane strains and (k_x, k_θ, $k_{x\theta}$) are the curvatures.

If in a filament-wound cylinder, wherein the kth lamina is bounded by the surfaces $Z = h_{k-1}$ and $Z = h_k$, the force and moment equations are given as:

$$\begin{bmatrix} N_x \\ N_\theta \\ N_{x\theta} \end{bmatrix} = \sum_{k=1}^{n}\int_{h_{k-1}}^{h_k}\begin{bmatrix} \sigma_x \\ \sigma_\theta \\ \sigma_{x\theta} \end{bmatrix} dZ \quad (5)$$

$$\begin{bmatrix} M_x \\ M_\theta \\ M_{x\theta} \end{bmatrix} = \sum_{k=1}^{n}\int_{h_{k-1}}^{h_k}\begin{bmatrix} \sigma_x \\ \sigma_\theta \\ \sigma_{x\theta} \end{bmatrix} Z dZ \quad (6)$$

where n, Z and (σ_x, σ_θ, $\sigma_{x\theta}$) are the number of laminae, distance from midplane, and stresses. The integration can be rearranged to take advantage of the fact that the stiffness matrix for the lamina is constant within the lamina. The stiffness matrix for a lamina varies only if the lamina has temperature-dependent properties and a temperature gradient exists across the lamina.

When the filament-wound cylinder has biaxial pressure loading, the constituent equations, using the N matrix has the following form [9]:

$$\begin{bmatrix} N_x \\ N_\theta \\ N_{x\theta} \end{bmatrix} = \begin{bmatrix} \frac{PR}{2} \\ PR \\ 0 \end{bmatrix} \quad (7)$$

where P and R are the internal pressure and radius of the filament-wound cylinder.

During biaxial pressure loading, only fibres can support the load, because maximum stress is concentrated in the resin area. From Fig. 1b, it is clear that the crack travels along the fibre. This does not result in a through-crack or the final failure of the filament-wound cylinder. The final failure of the cylinder is only possible when the fibres fail, and the maximum pressure, P_{max}, will be given as

$$\tau_{max} = \frac{N_\theta - N_x}{2t} = \frac{P_{max}R}{4t} \quad (8)$$

where t is the thickness of the cylinder.

However, there will be no further shear resistance in the interlaminar face, and shear resistance will be there in only half the area. Therefore, the burst pressure will drop to

$$P_b = \frac{4t\tau}{d} \quad (9)$$

where τ is the shear resistance.

The ratio of ultimate tensile strength to shear resistance or strength of GRP composites is given as [10]:

$$\frac{\sigma_u}{\tau} = 3.43 \quad (10)$$

Vary and Lark [4] have determined the relation between

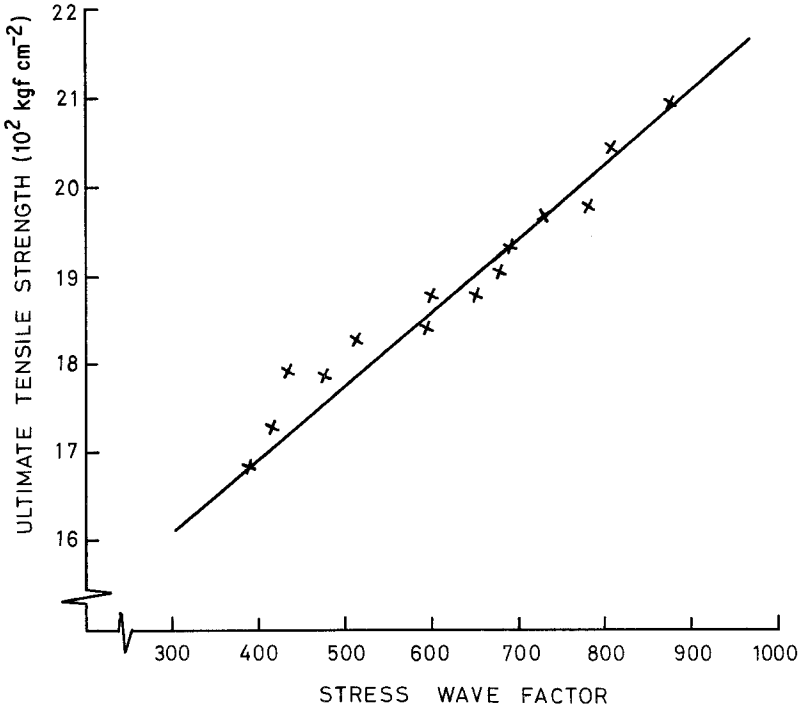

Figure 2 A plot of the ultimate tensile strength against the stress wave factor of GRP composites.

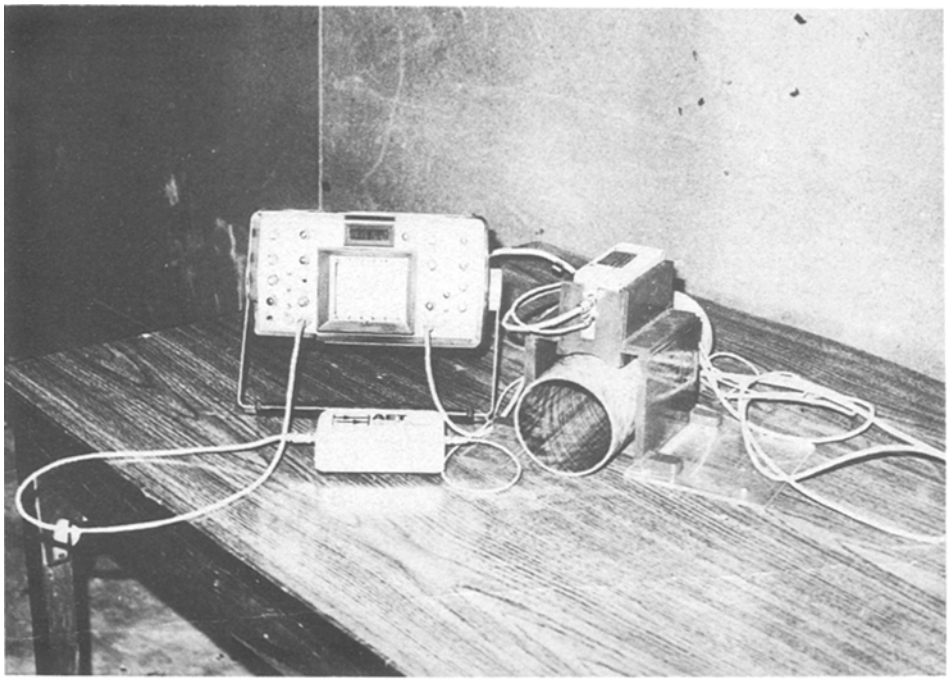

Figure 3 Photograph of the experimental acousto-ultrasonics testing apparatus.

the ultimate tensile strength of fibre composites and the stress wave factor. It may also be observed from Fig. 2 that the ratio of ultimate tensile strength of the GRP composite to the stress wave factor is given as

$$\frac{\sigma_u}{S_w} = 3.67 \quad (11)$$

From Equations 9, 10 and 11, we get

$$P_b = m \frac{t}{d} S_w \quad (12)$$

where $m = 4.28$ and is a material parameter. From Equation 12 one may substitute the values of internal diameter and thickness of the cylinder to obtain a theoretical curve between the burst pressure of GRP cylinders and the stress wave factor.

3. Experimental work

GRP cylinders about 370 mm long, with an inside diameter of 104 mm and a wall thickness of 4 mm (five double filament-wound layers, winding angle 46°) were used for the pressure tests.

The instrumentation used for evaluating the ultimate performance of GRP cylinders was an acousto-ultrasonic apparatus (Model, AET-206 AU). It is composed of three main sections: a pulser section, an acoustic emission section, and a display section. Using a broad band transducer, the pulser section injects ultrasonic pulses into the composite material. Each pulse produces simulated stress waves that resemble acoustic emission (AE) events. The piezoelectric acoustic emission sensor probe, 375 kHz resonant frequency, is used to receive the transmitted stress wave. A broadband 40 dB preamplifer including a band pass filter frequency is matched to the AE sensor. The ultrasonic waves input to the material under test is in the form of well-defined discrete pulses. These ultrasonic waves are modulated/dampened differently by different materials and also by different features in the same material.

The stress wave factor readings were obtained at different places on GRP cylinders, when the noise interference was minimum and where a good contact was obtained between the AET probe and the surface of the GRP cylinder using petroleum jelly as a couplant. The sensor fixture was pressed firmly against the GRP cylinder. Changes in pressure were avoided during the time the pulser was activated. This reduced

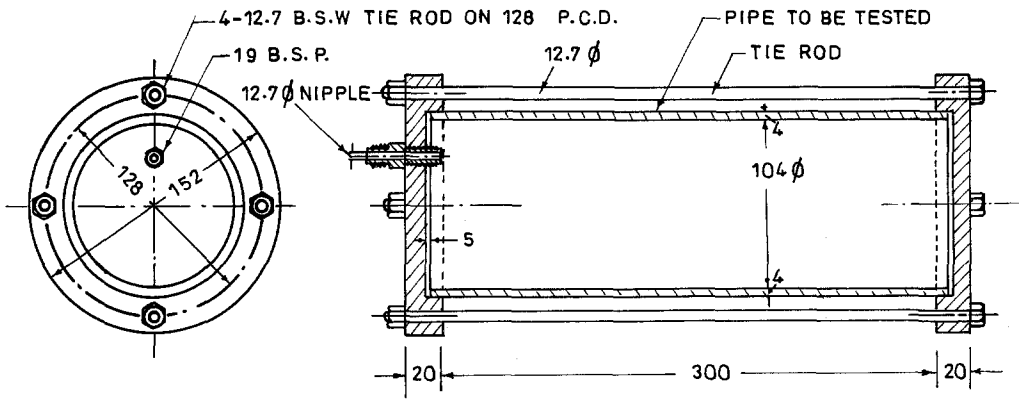

Figure 4 GRP tube for pressure testing (all dimensions in mm).

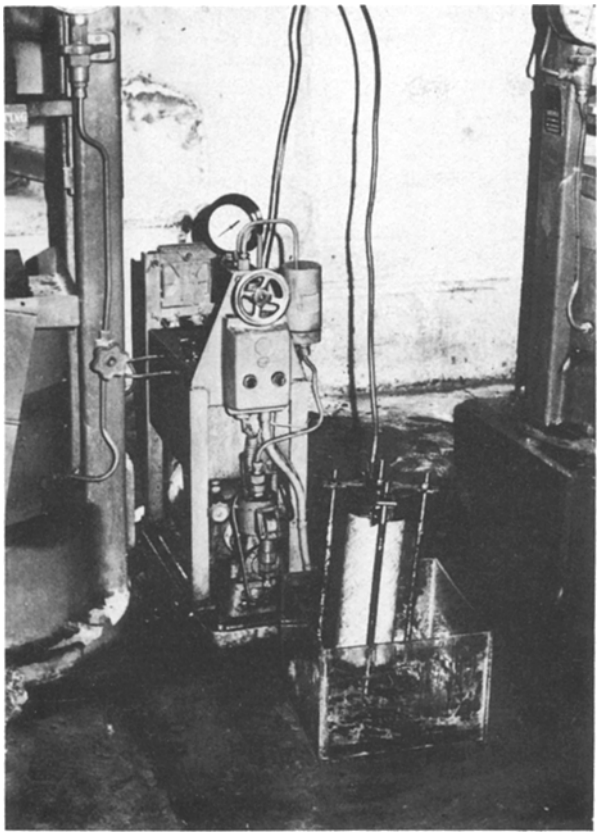

Figure 5 Photograph of the experimental pressure testing apparatus on the compression machine.

the chance of erroneous acoustic signals emanating from the fixture itself or from friction noises caused by the sensor sliding over the GRP cylinder. A photograph of the stress wave factor measurements is shown in Fig. 3. The lowest value of the stress wave factor for each GRP cylinder was noted and the area having the lowest stress wave factor was encircled with a dye-pen.

To protect the ends of the pipe sections, large collars were wound on each end to retain plugs. To seal the pipes under internal pressure, steel plugs with O-rings were inserted. During pressure tests in which the GRP cylinder was unrestrained, the plugs were held by split steel flanges bolted around the collars as shown in Fig. 4. Using a proper pressure pack and proper fixtures for holding the GRP cylinders, the cylinders were pressure tested on a compression machine, to obtain their burst pressure. A photograph showing an overall view of the pressure testing machine is shown in Fig. 5. The volume fractions of each GRP cylinder were obtained by burn-off methods.

4. Results and discussion

It was observed that GRP cylinders under test invariably failed within the prescribed region (i.e. within the area which was previously encircled with the dye-pen), having the lowest value of the stress wave factor, because the lowest value of stress wave factor governs the weakest spot. A plot (Fig. 6) showing the relationship between burst pressure and stress wave factor was then obtained. It was noted that the values of stress wave factor vary at low burst pressure, because the lowest value of the stress wave factor governs the poorest quality of the GRP cylinder. There are also many physical parameters, such as resin crazing, delamination, microvoids, etc., that may affect the quality of GRP cylinders.

To obtain the best fit line and confidence level between burst pressure and stress wave factor of the GRP cylinders, data were fed into the ICL 1900 computer using a simple library program. Fig. 6 shows the correlation curves. A Student t-value of 5.4 for the regression coefficient is moderately high, indicating that the coefficient cannot be zero. The correlation table concludes that the greatest

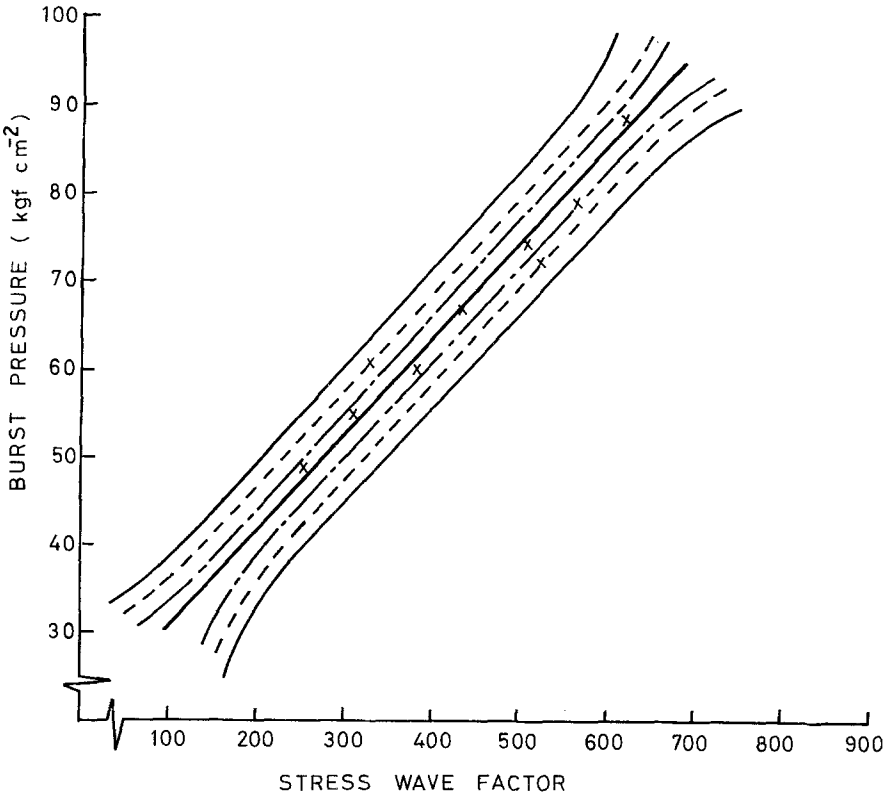

Figure 6 Correlation curves indicating: —— the best fit; – – – 90% confidence level; – – – 95% confidence level; —— 99% confidence level.

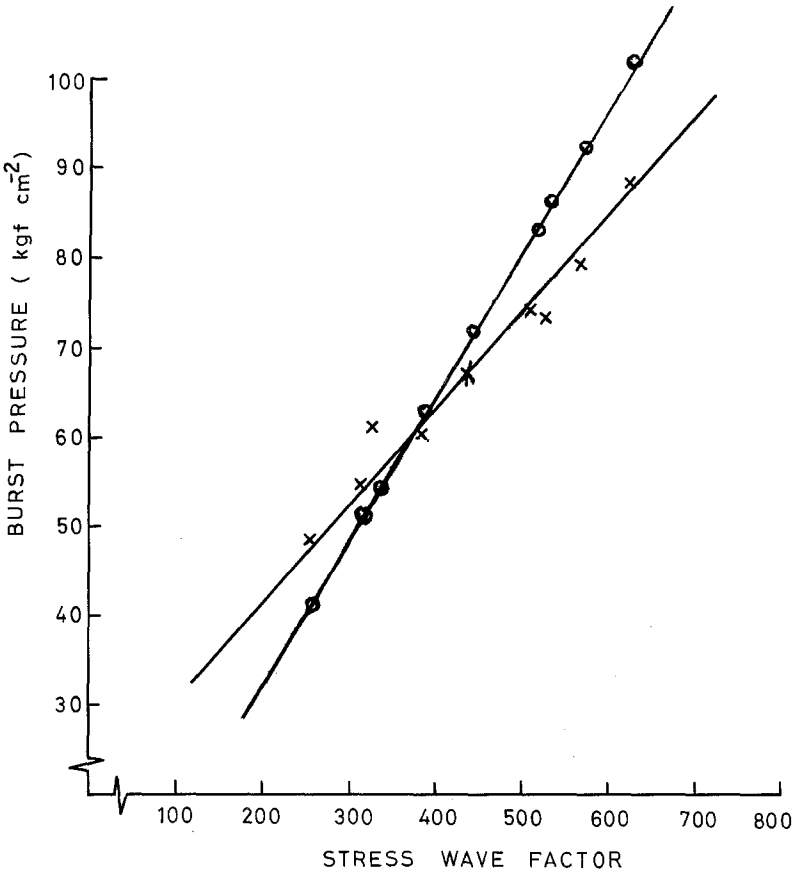

Figure 7 Comparison of (×) enperimental and (○) theoretical values of burst pressure with the stress wave factor of GRP composites.

correlation (0.965) exists between burst pressure and stress wave factor of GRP cylinders. From the figure it is clear that larger stress wave factor will exhibit a greater burst pressure of the GRP cylinder.

The theoretical values of burst pressure of GRP cylinders having different stress wave factors were obtained using Equation 12. Fig. 7 shows a comparison of theoretical and experimental curves for the burst pressure of GRP cylinders. From the figure, it is clear that the slope of each curve is approximately the same. From the experimental results it is clear that the value of the stress wave factor fluctuates at the lower value of burst pressure, because the lower values of stress wave factor indicates that more defects are present in the cylinder. The theoretical burst pressure of GRP cylinders has been found to be in good agreement with the experimental values. Hence, one can non-destructively evaluate the burst pressure of GRP cylinders by measuring the stress wave factor.

5. Conclusion

The experiments carried out have conclusively shown that it is possible to non-destructively evaluate the burst pressure of a GRP cylinder. The non-destructive evaluation of this property will allow designers to reduce the factor of safety and thus obtain an economical design of GRP cylinders. The burst pressure of a GRP composite cylinder is obtained from following expression:

$$P_b = \frac{mtS_w}{d}$$

Acknowledgement

The author wishes to acknowledge provision of research facilities by the Department of Mechanical Engineering, Institute of Technology, Banaras Hindu University, Varanasi, India.

References

1. A. VARY, "Recent Advances in Acousto-ultrasonic Measurements of composite mechanical properties", 1979 ASNT Fall Conference, St. Louis, Missouri, October 1979.
2. A. VARY and K. J. BOWLES, "Ultrasonic evaluation of the strength of unidirectional graphite-polyimide composites", NASA, Lewis Research Center, Cleveland, Ohio, NASA TM X-73646, April 1977.
3. A. VARY and K. J. BOWLES, *Polym. Eng. Sci.* **19** (1979) 373.
4. A. VARY and R. F. LARK, *J. Test. Eval.* **7** (1979) 185.
5. H. J. SCHWALBE, "Acoustic emission as an aid for inspecting GFRP pressure tubes", Proceedings of the 2nd International Conference on Composite materials, TCCM-2, Toronto, Canada, (1978) p. 1099.
6. A. T. GREEN, "Evaluation of Composite structures by stress wave factor and acoustic emission", Symposium on Reliability through NDE, Pune, India (1982).
7. A. VARY, *J. Mater. Eval.* **40** (1982) 650.
8. V. K. SRIVASTAVA and R. PRAKASH, "NDE of hybrid glass/carbon fibre composites using Acousto-ultrasonics technique", Proceedings of the National Conference on NDE, Indian Institute of Science, Bangalore, March (1984).
9. M. W. K. ROSENOW, *Composites* **15** (1984) 144.
10. R. SONNEBORN, "Fibrous glass reinforcement, Modern plastics Encyclopedia" (McGraw-Hill, New York, 1962) p. 565.

Received 4 September
and accepted 18 December 1985